Chen *et al. Geosci. Lett. (2017) 4:30*
https://doi.org/10.1186/s40562-017-0096-1

Geoscience Letters

RESEARCH LETTER

Open Access

Ellerman bombs observed with the new vacuum solar telescope and the atmospheric imaging assembly onboard the solar dynamics observatory

Yajie Chen[1], Hui Tian[1*], Zhi Xu[2], Yongyuan Xiang[2], Yuliang Fang[2] and Zihao Yang[1]

Abstract

Ellerman bombs (EBs) are believed to be small-scale reconnection events occurring around the temperature minimum region in the solar atmosphere. They are often identified as significant enhancements in the extended Hα wings without obvious signatures in the Hα core. Here we explore the possibility of using the 1700 Å images taken by the Atmospheric Imaging Assembly (AIA) onboard the Solar Dynamics Observatory (SDO) to study EBs. From the Hα wing images obtained with the New Vacuum Solar Telescope (NVST) on 2015 May 2, we have identified 145 EBs and 51% of them clearly correspond to the bright points (BPs) in the AIA 1700 Å images. If we resize the NVST images using a linear interpolation to make the pixel sizes of the AIA and NVST images the same, some previously identified EBs disappear and about 71% of the remaining EBs are associated with BPs. Meanwhile, 66% of the compact brightenings in the AIA 1700 Å images can be identified as EBs in the Hα wings. The intensity enhancements of the EBs in the Hα wing images reveal a linear correlation with those of the BPs in the AIA 1700 Å images. Our study suggests that a significant fraction of EBs can be observed with the AIA 1700 Å filter, which is promising for large-sample statistical study of EBs as the seeing-free and full-disk SDO/AIA data are routinely available.

Background

Ellerman bombs (EBs) are intense transient brightenings in the extended Hα wings without obvious signatures in the Hα core (Ellerman 1917). They are often believed to be small-scale reconnection events occurring in the low atmosphere of solar active regions (Pariat et al. 2007; González et al. 2013). However, recent observations clearly reveal that they are also present in the quiet-Sun regions (van der Voort et al. 2016; Nelson et al. 2017). While some studies suggested that EBs form in the low chromosphere (e.g., Schmieder et al. 2004), recent high-resolution observations indicated that they just occur in the photosphere (e.g., Watanabe et al. 2011; Vissers et al. 2013). EBs typically last for 10–20 min (Kurokawa et al. 1982; Qiu et al. 2000) and they have a size on the order of 1″ (Dunn and Zirker 1973; Dara et al. 1997).

EBs are usually studied using the Hα data obtained by ground-based telescopes. However, ground-based observations often suffer from varying seeing conditions. As a result, only a small number of high-quality EB datasets have been acquired in the past. Such a limitation largely hampers the investigation of EBs, especially large-sample statistical studies of EBs. Qiu et al. (2000) first noticed that some EBs have signatures in the 1600 Å images obtained with the transition region and coronal explorer (TRACE, Handy et al. 1999). More recently, it has also been found that some EBs correspond to small-scale compact brightenings in the 1700 Å images taken by the Atmospheric Imaging Assembly (AIA, Lemen et al. 2012) onboard the solar dynamics observatory (SDO) (Vissers et al. 2013; Tian et al. 2016; Zhao et al. 2017; Toriumi et al. 2017). After the launch of the Interface Region Imaging Spectrograph (IRIS; De Pontieu et al. 2014) mission, EBs

*Correspondence: huitian@pku.edu.cn
[1] School of Earth and Space Sciences, Peking University, Beijing 100871, China
Full list of author information is available at the end of the article

have received intensive investigation, as IRIS observations appear to reveal unexpected heating of EBs to a few tens of thousands of kelvin (e.g., Peter et al. 2014; Vissers et al. 2015; Cho et al. 2015; Tian et al. 2016; Grubecka et al. 2016). However, it is still under debate whether such intense heating is directly caused by the EBs or not (e.g., Lei et al. 2016; Reid et al. 2017; Berlicki and Heinzel 2014; Fang et al. 2017; Hong et al. 2017; Danilovic 2017; Hansteen et al. 2017).

Here we analyze the data taken by SDO/AIA and the Chinese 1-m New Vacuum Solar Telescope (NVST, Liu 2014), and perform the first statistical study on the visibility of EBs in AIA 1700 Å images. Our analysis results demonstrate that many EBs can be observed with the AIA 1700 Å filter, which has significant implication for large-sample statistical studies of EBs.

Observations and data analysis

We use the dataset acquired by NVST from 01:11 to 03:59 UT on 2015 May 2, which is the same dataset used by Tian et al. (2016). The pointing coordinate is (− 814″, − 222″) in this observation. The NVST data include images of the Hα core, blue wing at − 1 Å and red wing at + 1 Å. The time cadence for each passband is ~ 50 s, and the spatial pixel size is 0.167 arcsec. The blue wing images are not used in this study as some EBs are obscured by surges or spicules (Tian et al. 2016).

These Hα images are used to identify EBs. We first take the Hα red wing images and select those pixels with intensity exceeding 4σ (σ is the standard derivation of the intensity) above the average in at least two continuous images. If there is no obvious increase at the same pixels in the Hα core images, these pixels will be identified as pixels of EB candidates. Any four contiguous pixels of EB candidates that appear in at least two consecutive images will be counted as one EB. Using this method, we have identified 145 EBs from our NVST observation.

The AIA 1700 Å images have a cadence of 24 s and a pixel size of ~ 0.6″. The coalignment between the NVST images and AIA 1700 Å images is achieved by matching the locations of some commonly observed compact brightenings in the Hα wing images and AIA 1700 Å images. After coalignment, we extract the data cube of a small region corresponding to the field of view (FOV) of the NVST observation from the full-disk 1700 Å images. Bright pixels in the AIA 1700 Å images are flagged by using an intensity threshold of 3.5σ above the average intensity. These pixels are defined as pixels of the candidates of 1700 Å bright points (BPs). Any four contiguous pixels of BP candidates that appear in at least two consecutive images will be counted as one BP. Using this method, we have identified 125 BPs from the AIA 1700 Å images obtained during the NVST observation period.

Figure 1 shows a snapshot of the NVST Hα red wing and SDO/AIA 1700 Å observations. The field of view is 75″ × 75″. The red and blue contours represent locations where the intensities exceed the thresholds mentioned above. So the blue contours indicate BPs in the 1700 Å images, while the red contours mark potential candidates of EBs. Only those red contours within which the Hα core intensities do not show an obvious increase will be identified as EBs. As an example, the identified EBs and BPs detected at 01:12 UT in a smaller region are shown in Fig. 2. In the following, we will examine which EBs are found at the locations of BPs, and how many BPs are found at the locations of EBs.

Results and discussion

We find that 74 EBs (51% of the 145 EBs identified) can be clearly recognized as BPs in the AIA 1700 Å images. Figure 2 shows some examples of these BP-related EBs. These EBs are generally the stronger and larger EBs. As the spatial resolution of NVST is much higher than that of AIA, it is likely that some small-scale and weak EBs also have weak 1700 Å emission that is below the intensity threshold we use to identify BPs. We have also resized the NVST images using a linear interpolation to make the pixel sizes of AIA and NVST images the same. Using the resized NVST images, we find that some previously identified EBs disappear and that about 71% of the remaining EBs correspond to BPs in the AIA 1700 Å images.

On the other hand, 66 BPs (53% of the 125 BPs) in the AIA 1700 Å images correspond to identified EBs in the Hα wing images. If we do not consider the large-scale (~ 5″) BPs in the AIA 1700 Å images, the percentage will be 66%. It appears that these large-scale brightenings are caused by microflares or other phenomena in the chromosphere rather than EBs.

Qiu et al. (2000) found that most EBs that are related to UV enhancement are located at the boundaries of unipolar magnetic areas. In our observation the target active region is close to the east limb. Thus, the measurement of magnetic field is not reliable. Because of this observational limitation, it is difficult to tell whether different magnetic field structures are associated with the EBs showing signatures in the AIA 1700 Å images and those showing no detectable signatures in AIA 1700 Å images.

Figure 3 presents scatter plots of the relationship between the lifetime and intensity of EBs in Hα wing images, as well as the intensity of EBs in Hα wing and AIA 1700 Å images. Note that the intensity here refers to the intensity at the brightest pixel of an EB or BP (within each contour). The first scatter plot shows a clear positive correlation between the intensity and lifetime of EBs. This means that brighter EBs often have longer lifetimes, possibly suggesting that EBs with higher energies

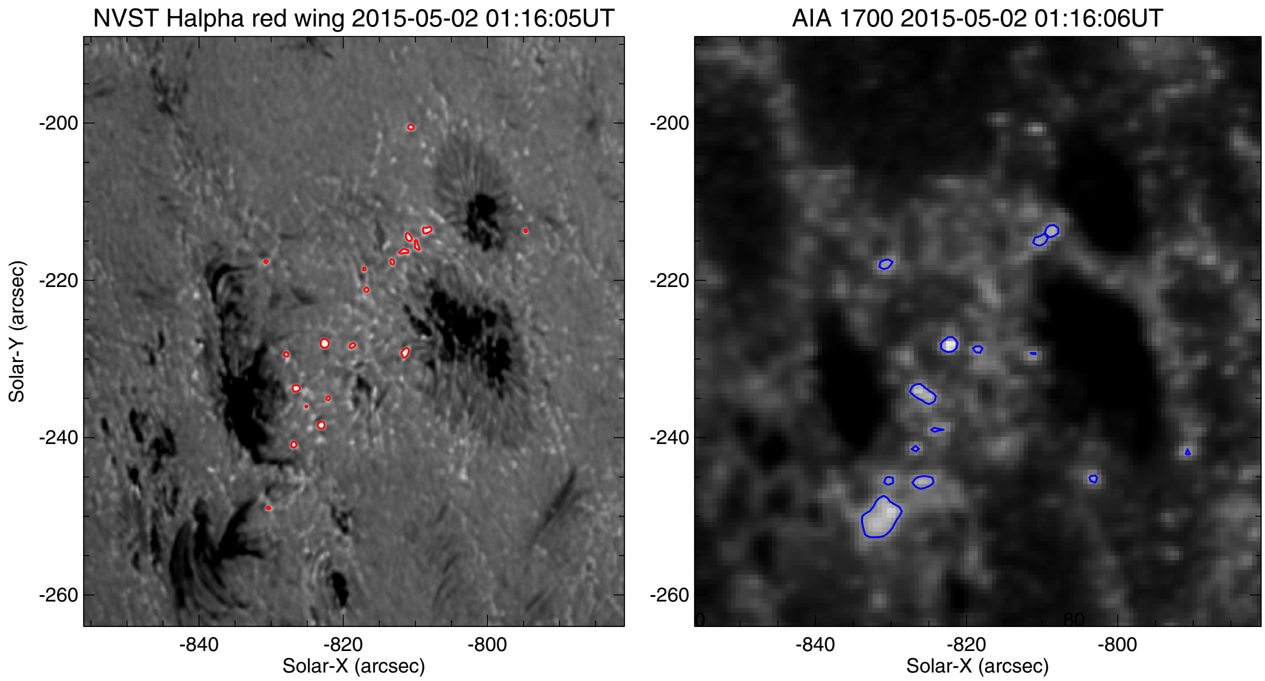

Fig. 1 Images of Hα red wing (left panel) and 1700 Å (right panel) taken at 01:12 UT on 2015 May 2. The red and blue contours mark the brightest pixels in the Hα red wing and 1700 Å images, respectively, using the intensity thresholds mentioned in "Observations and data analysis" section

generally have longer lifetimes. The second scatter plot shows a tendency that the intensities of EBs in Hα wing images have a positive correlation with the intensities at the corresponding pixels in AIA 1700 Å images. We also divide the Hα wing intensities into several bins with a bin size of 400, then calculate the average 1700 Å intensity in each bin. A general trend of larger 1700 Å intensity with increasing Hα wing intensity can be clearly seen.

Figure 4 shows the distributions of the intensities and lifetimes for the BP-related EBs and EBs which are not related to BPs. Obviously, EBs that are not associated with BPs in the AIA 1700 Å images have smaller intensities and shorter lifetimes compared to the BP-related EBs. The lifetimes of most EBs are less than 20 min, which is consistent with the typical lifetime of EBs (10–20 min) reported in previous studies (Kurokawa et al. 1982; Qiu et al. 2000). As some EBs could repeatedly occur around the same locations and some EBs may disappear and recur within the time interval between two continuous exposures, the estimated lifetimes of EBs might be larger than the real lifetimes.

Summary

Using joint observations of NVST and SDO/AIA, we have performed the first statistical study on the visibility of EBs in the AIA 1700 Å images. We have identified 145 EBs from the H wing images, and found that 74 of them (51%) can be clearly identified as BPs in the AIA 1700 Å images. Most of these 74 EBs are relatively large and strong EBs. We have also resized the NVST images using a linear interpolation to make the pixel sizes of the AIA and NVST images the same. After doing this we have re-identified EBs in the resized NVST images, and found that 71% of them are associated with BPs. Meanwhile, we have identified 125 BPs from the AIA 1700 Å images, with 66 of them (53%) corresponding to EBs in the H wing images. This percentage becomes 66% if we exclude large-scale BPs that are likely caused by microflares rather than EBs in the AIA 1700 Å images. The intensities of EBs in the Hα wing images reveal a linear correlation with the AIA 1700 Å intensities.

Our results indicate that most small-scale, compact, and transient brightenings in the AIA 1700 Å images can

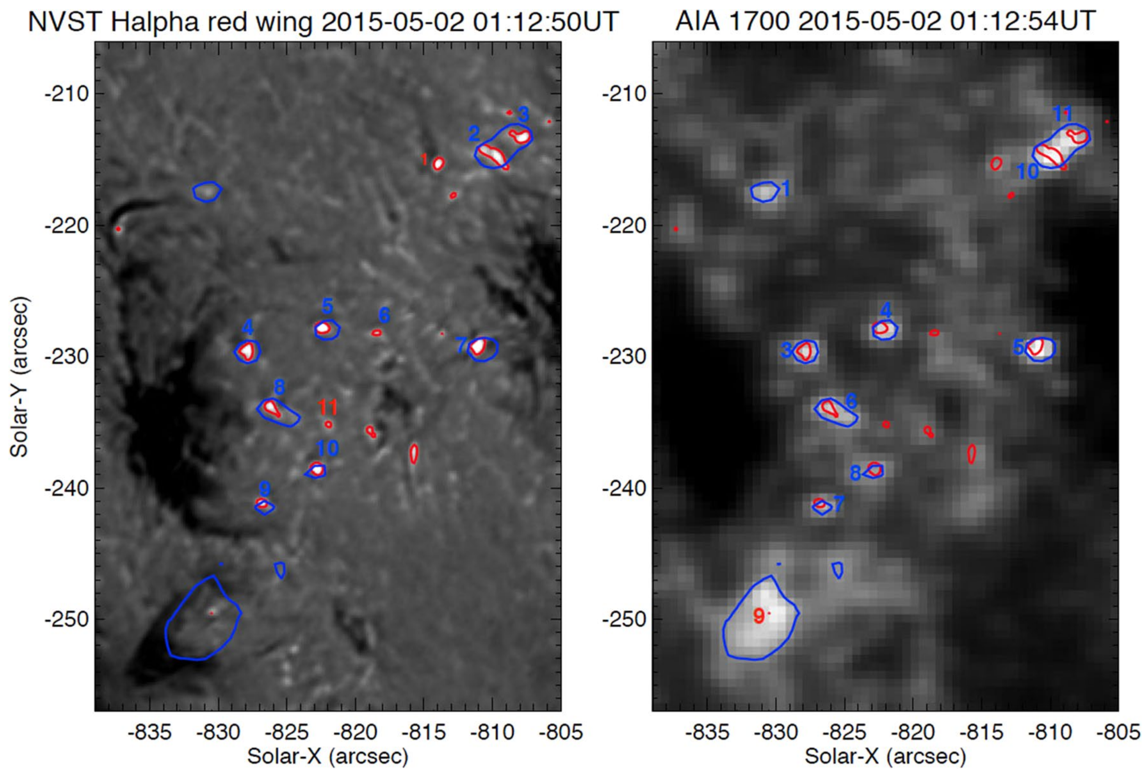

Fig. 2 Images of Hα red wing (left panel) and 1700 Å (right panel) taken at 01:12 UT on 2015 May 2. Only part of the full field of view is shown here. The red and blue contours mark the brightest pixels in the Hα red wing and 1700 Å images, respectively, using the intensity thresholds mentioned in "Observations and data analysis" section. Identified EBs are indicated by the numbers in the left image, where the blue and red numbers indicate EBs that are related or not related to BPs, respectively. In the right image, the blue and red numbers indicate BPs that are related or not related to EBs, respectively

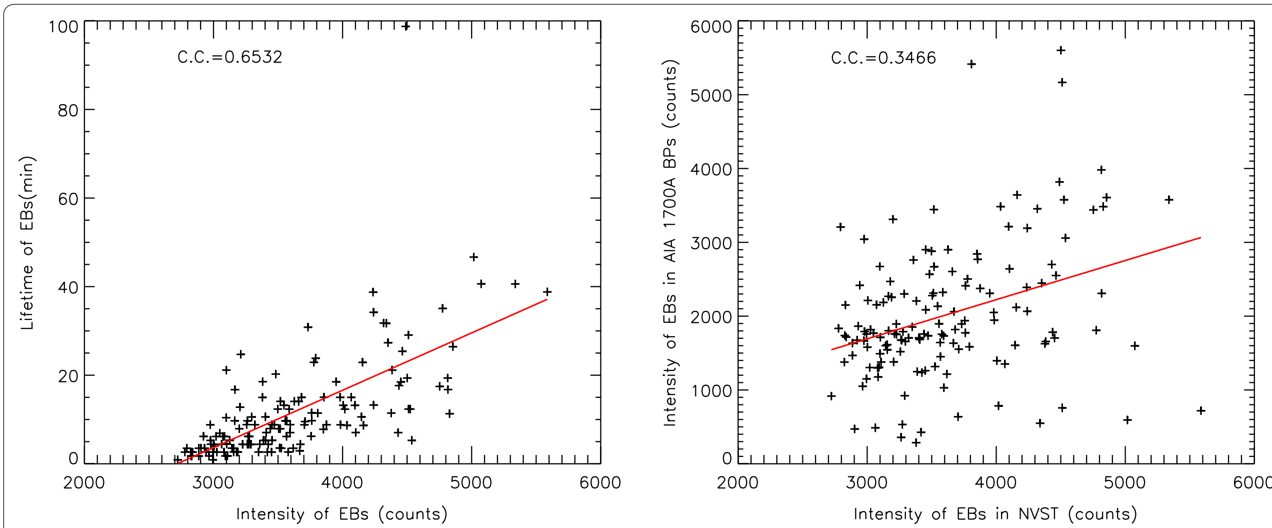

Fig. 3 Left panel: scatter plot depicting the relationship between the intensity and lifetime of EBs identified from the Hα wing images. Right panel: scatter plot depicting the relationship between EB intensity in Hα wing and AIA 1700 Å images. Each red diamond represents the average 1700 Å intensity in each bin of Hα wing intensity. Red lines represent the results from a linear fitting

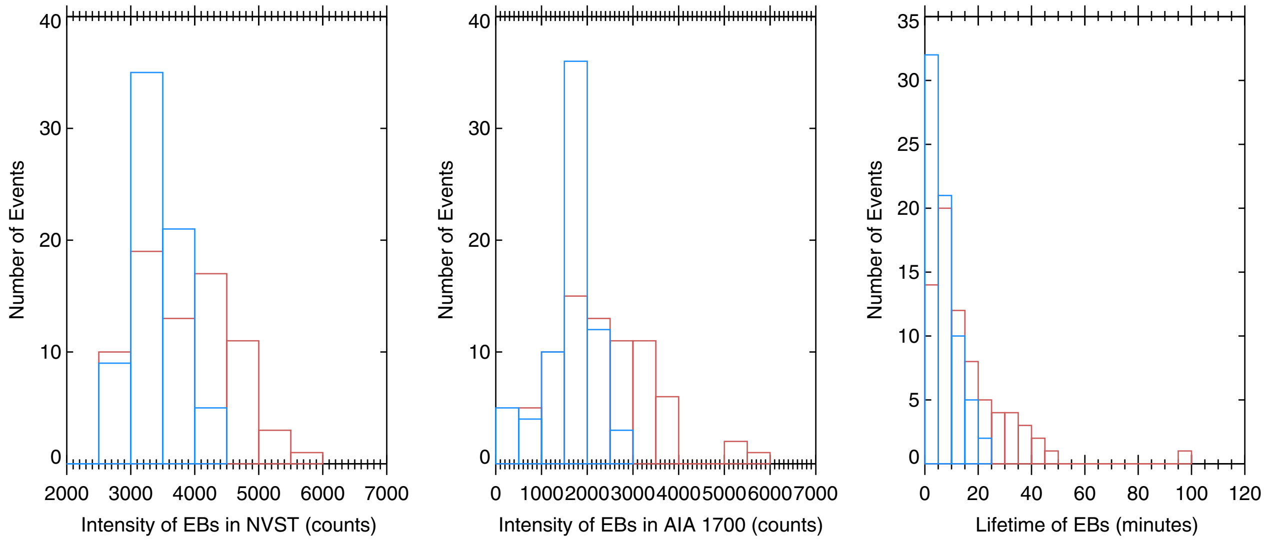

Fig. 4 Distributions of the intensities of EBs in the Hα wing images, the AIA 1700 Å intensities at the locations of EBs, and the lifetimes of EBs derived from Hα wing observations. The red and blue histograms represent the results for the BP-related EBs and EBs that are not related to BPs, respectively

be identified as EBs, which is promising for large-sample statistical study of EBs as the seeing-free and full-disk SDO/AIA data are routinely available.

Authors' contributions
YC performed the data analysis. HT initiated this study. ZX, YX, and YF carried out the NVST observation and processed the NVST data. ZY participated in the discussion and draft writing. All authors read and approved the final manuscript.

Author details
[1] School of Earth and Space Sciences, Peking University, Beijing 100871, China. [2] Yunnan Observatories, Chinese Academy of Sciences, 396 Yangfangwang, Guandu District, Kunming 650216, China.

Acknowledgements
H.T. thanks ISSI Bern for the support to the team "Solar UV bursts—a new insight to magnetic reconnection." We thank Hardi Peter for helpful discussion and constructive suggestions.

Competing interests
The authors declare that they have no competing interests.

Availability of data and materials
The NVST data analyzed in this paper are archived at the Fuxian Solar Observatory, Yunnan Observatories, Chinese Academy of Sciences, and they can be accessed at the observatory website of http://fso.ynao.ac.cn/dataarchive_ql.aspx. The publicly available SDO/AIA data (including the data used in this study) are archived at Joint Science Operations Center (http://jsoc.stanford.edu/AIA/AIA_jsoc.html).

Consent for publication
Not applicable.

Ethics approval and consent to participate
Not applicable.

Funding
This work is supported by NSFC Grants 11790304, 11473064, and 41574166, the Recruitment Program of Global Experts of China, and the Max Planck Partner Group program.

Publisher's Note
Springer Nature remains neutral with regard to jurisdictional claims in published maps and institutional affiliations.

Received: 31 August 2017 Accepted: 5 December 2017
Published online: 12 December 2017

References
Berlicki A, Heinzel P (2014) Observations and nlte modeling of Ellerman bombs. Astron Astrophys 567(2):3733–3741
Cho IH, Cho KS, Bong SC, Lim EK, Kim RS, Choi S et al (2015) Statistical comparison between pores and sunspots by using SDO/HMI. Astrophys J 811(1):49
Danilovic S (2017) Simulating Ellerman bomb-like events. Astron Astrophys 601. https://doi.org/10.1051/0004-6361/201730403
Dara HC, Alissandrakis CE, Zachariadis TG, Georgakilas AA (1997) Magnetic and velocity field in association with Ellerman bombs. Astron Astrophys 322(2):653–658
De Pontieu B, Title AM, Lemen JR, Kushner GD, Akin DJ, Allard B et al (2014) The interface region imaging spectrograph (IRIS). Sol Phys 289(7):2733–2779
Dunn RB, Zirker JB (1973) The solar filigree. Sol Phys 33(2):281–304
Ellerman F (1917) Solar hydrogen. Astrophys J 46:298
Fang C, Hao Q, Ding MD, Li Z (2017) Can the temperature of Ellerman bombs be more than 10 000 K? Res Astron Astrophys 17(4):1–6
González NB, Danilovic S, Kneer F (2013) On the structure and dynamics of Ellerman bombs. Astron Astrophys 557:16
Grubecka M, Schmieder B, Berlicki A, Heinzel P, Dalmasse K, Mein P (2016) Height formation of bright points observed by IRIS in Mg II line wings during flux emergence. Astron Astrophys 593:A32
Handy BN, Acton LW, Kankelborg CC, Wolfson CJ, Akin DJ, Bruner ME, Parkinson C et al (1999) The transition regions and coronal explorer. White paper for 2010 decadal study. Sol Phys 187:229–260
Hansteen VH, Archontis V, Pereira TMD, Carlsson M, Rouppe VDVL, Leenaarts J (2017) Bombs and flares at the surface and lower atmosphere of the sun. Astrophys J 839(1):22
Hong J, Carlsson M, Ding MD (2017) Radyn simulations of non-thermal and thermal models of Ellerman bombs. Astrophys J 845:144

Kurokawa H, Kawaguchi I, Funakoshi Y, Nakai Y (1982) Morphological and evolutional features of Ellerman bombs. Sol Phys 79(1):77–84
Lei N, Lin J, Roussev II, Schmieder B (2016) Heating mechanisms in the low solar atmosphere through magnetic reconnection in current sheets. Astrophys J 832(2):195
Lemen JR, Title AM, Akin DJ et al (2012) The atmospheric imaging assembly (AIA) on the solar dynamics observatory (SDO). Sol Phys 275:17
Liu Z (2014) New vacuum solar telescope and observations with high resolution. Res Astron Astrophys 14(6):705–718
Nelson CJ, Freij N, Reid A, Oliver R, Mathioudakis M, Erdélyi R (2017) IRIS burst spectra co-spatial to a quiet-sun Ellerman-like brightening. Astrophys J 845:16
Pariat E, Schmieder B, Berlicki A, Deng Y, Mein N, Ariste AL, et al. (2007) Spectrophotometric analysis of Ellerman bombs in the Ca II, Hα, and UV range. Astron Astrophys 473(1):279–289
Peter H, Tian H, Curdt W, Schmit D, Innes D, De PB et al (2014) Hot explosions in the cool atmosphere of the sun. Science 346(6207):1255726
Qiu J, Ding MD, Wang H, Denker C, Goode PR (2000) Ultraviolet and Hα emission in Ellerman bombs. Astrophys J Lett 544(2):L157–L161
Reid A, Mathioudakis M, Kowalski A, Doyle JG, Allred JC (2017) Solar Ellerman bombs in 1-D radiative hydrodynamics. Astrophys J 835:L37
Schmieder B, Rust DM, Georgoulis MK, Démoulin P, Bernasconi PN (2004) Emerging flux and the heating of coronal loops. Astrophys J 601(1):530
Tian H, Xu Z, He J, Madsen C (2016) Are iris bombs connected to Ellerman bombs? Astrophys J 824(2):96
Toriumi S, Katsukawa Y, Cheung MCM (2017) Various local heating events in the earliest phase of flux emergence. Astrophys J 836(1):63
van der Voort LH, Rutten RJ, Vissers GJ (2016) Reconnection brightenings in the quiet solar photosphere. Astron Astrophys 592:A100
Vissers GJM, van der Voort LHM, Rutten RJ (2013) Ellerman bombs at high resolution: II. Visibility, triggering and effect on upper atmosphere. Astrophys J 774(774):702–713
Vissers GJM, Luc HM, van der Voort R, Rutten RJ, Carlsson M, Pontieu BD (2015) Ellerman bombs at high resolution III. Simultaneous observations with IRIS and SST. Astrophys J 812(1):11
Watanabe H, Vissers G, Kitai R, Voort LRVD, Rutten RJ (2011) Ellerman bombs at high resolution: I. Morphological evidence for photospheric reconnection. Astrophys J 736(1):71
Zhao J, Schmieder B, Li H, Pariat E, Zhu X, Feng L et al (2017) Observational evidence of magnetic reconnection for brightenings and transition region arcades in IRIS observations. Astrophys J 823(1):62